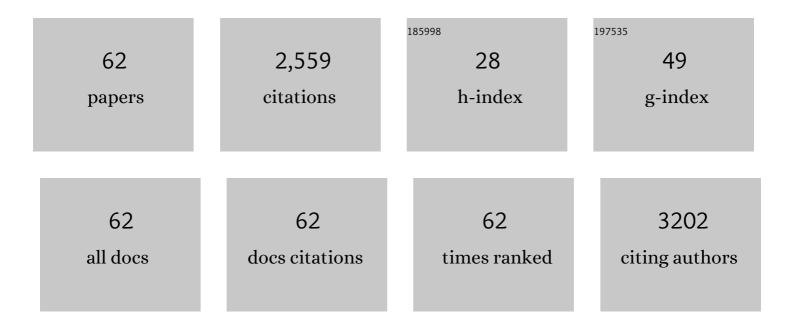
## **Guangliang Ding**

List of Publications by Year in descending order

Source: https://exaly.com/author-pdf/7796876/publications.pdf Version: 2024-02-01



#	Article	IF	CITATIONS
1	The role of the parenchymal vascular system in cerebrospinal fluid tracer clearance. European Radiology, 2023, 33, 656-665.	2.3	4
2	MRI Metrics of Cerebral Endothelial Cell–Derived Exosomes for the Treatment of Cognitive Dysfunction Induced in Aging Rats Subjected to Type 2 Diabetes. Diabetes, 2022, 71, 873-880.	0.3	2
3	Aging-Related Alterations of Glymphatic Transport in Rat: In vivo Magnetic Resonance Imaging and Kinetic Study. Frontiers in Aging Neuroscience, 2022, 14, 841798.	1.7	10
4	Cerebral endothelial cell-derived small extracellular vesicles enhance neurovascular function and neurological recovery in rat acute ischemic stroke models of mechanical thrombectomy and embolic stroke treatment with tPA. Journal of Cerebral Blood Flow and Metabolism, 2021, 41, 0271678X2199298.	2.4	12
5	Waste Clearance in the Brain. Frontiers in Neuroanatomy, 2021, 15, 665803.	0.9	32
6	MRI detection of impairment of glymphatic function in rat after mild traumatic brain injury. Brain Research, 2020, 1747, 147062.	1.1	31
7	Magnetic Resonance Imaging and Modeling of the Glymphatic System. Diagnostics, 2020, 10, 344.	1.3	21
8	Differences between normal and diabetic brains in middle-aged rats by MRI. Brain Research, 2019, 1724, 146407.	1.1	5
9	Diffuse white matter response in trauma-injured brain to bone marrow stromal cell treatment detected by diffusional kurtosis imaging. Brain Research, 2019, 1717, 127-135.	1.1	3
10	Modeling glymphatic system of the brain using MRI. NeuroImage, 2019, 188, 616-627.	2.1	46
11	Noninvasive measurement of renal blood flow by magnetic resonance imaging in rats. American Journal of Physiology - Renal Physiology, 2018, 314, F99-F106.	1.3	6
12	MRI investigation of glymphatic responses to Gdâ€DTPA infusion rates. Journal of Neuroscience Research, 2018, 96, 1876-1886.	1.3	23
13	White matter changes after stroke in type 2 diabetic rats measured by diffusion magnetic resonance imaging. Journal of Cerebral Blood Flow and Metabolism, 2017, 37, 241-251.	2.4	17
14	Impairment of the glymphatic system after diabetes. Journal of Cerebral Blood Flow and Metabolism, 2017, 37, 1326-1337.	2.4	194
15	Diffusion-Derived Magnetic Resonance Imaging Measures of Longitudinal Microstructural Remodeling Induced by Marrow Stromal Cell Therapy after Traumatic Brain Injury. Journal of Neurotrauma, 2017, 34, 182-191.	1.7	9
16	Chronic global analysis of vascular permeability and cerebral blood flow after bone marrow stromal cell treatment of traumatic brain injury in the rat: A long-term MRI study. Brain Research, 2017, 1675, 61-70.	1.1	4
17	Cell Treatment for Stroke in Type Two Diabetic Rats Improves Vascular Permeability Measured by MRI. PLoS ONE, 2016, 11, e0149147.	1.1	11
18	Persistent Cerebrovascular Damage After Stroke in Type Two Diabetic Rats Measured by Magnetic Resonance Imaging. Stroke, 2015, 46, 507-512.	1.0	35

GUANGLIANG DING

#	Article	IF	CITATIONS
19	Focal embolic cerebral ischemia in the rat. Nature Protocols, 2015, 10, 539-547.	5.5	73
20	An Analytical Model for Estimating Water Exchange Rate in White Matter Using Diffusion MRI. PLoS ONE, 2014, 9, e95921.	1.1	8
21	Intratumor distribution and test–retest comparisons of physiological parameters quantified by dynamic contrastâ€enhanced MRI in rat U251 glioma. NMR in Biomedicine, 2014, 27, 1230-1238.	1.6	20
22	Combination Treatment With N-Acetyl-Seryl-Aspartyl-Lysyl-Proline and Tissue Plasminogen Activator Provides Potent Neuroprotection in Rats After Stroke. Stroke, 2014, 45, 1108-1114.	1.0	22
23	Degree of corticospinal tract damage correlates with motor function after stroke. Annals of Clinical and Translational Neurology, 2014, 1, 891-899.	1.7	54
24	Perfusion and Diffusion Abnormalities of Multiple Sclerosis Lesions and Relevance of Classified Lesions to Disease Status. Journal of Neurology & Neurophysiology, 2013, s12, 12.	0.1	6
25	Comparison of Neurite Density Measured by MRI and Histology after TBI. PLoS ONE, 2013, 8, e63511.	1.1	19
26	MRI of Neuronal Recovery after Low-Dose Methamphetamine Treatment of Traumatic Brain Injury in Rats. PLoS ONE, 2013, 8, e61241.	1.1	17
27	Characterizing Brain Structures and Remodeling after TBI Based on Information Content, Diffusion Entropy. PLoS ONE, 2013, 8, e76343.	1.1	19
28	MRI Measurement of Angiogenesis and the Therapeutic Effect of Acute Marrow Stromal Cell Administration on Traumatic Brain Injury. Journal of Cerebral Blood Flow and Metabolism, 2012, 32, 2023-2032.	2.4	23
29	MRI Detects Brain Reorganization after Human Umbilical Tissue-Derived Cells (hUTC) Treatment of Stroke in Rat. PLoS ONE, 2012, 7, e42845.	1.1	27
30	Transplantation of Marrow Stromal Cells Restores Cerebral Blood Flow and Reduces Cerebral Atrophy in Rats with Traumatic Brain Injury: <i>In vivo</i> MRI Study. Journal of Neurotrauma, 2011, 28, 535-545.	1.7	43
31	MRI evaluation of axonal reorganization after bone marrow stromal cell treatment of traumatic brain injury. NMR in Biomedicine, 2011, 24, 1119-1128.	1.6	55
32	Longitudinal Magnetic Resonance Imaging of Sildenafil Treatment of Embolic Stroke in Aged Rats. Stroke, 2011, 42, 3537-3541.	1.0	29
33	Cerebral tissue repair and atrophy after embolic stroke in rat: A magnetic resonance imaging study of erythropoietin therapy. Journal of Neuroscience Research, 2010, 88, 3206-3214.	1.3	28
34	Effects of Administration Route on Migration and Distribution of Neural Progenitor Cells Transplanted into Rats with Focal Cerebral Ischemia, an MRI Study. Journal of Cerebral Blood Flow and Metabolism, 2010, 30, 653-662.	2.4	152
35	Quantitative Analysis of Clinical Dynamic Contrast-enhanced MR Imaging for Evaluating Treatment Response in Human Breast Cancer. Radiology, 2010, 257, 47-55.	3.6	33
36	MRI Identification of White Matter Reorganization Enhanced by Erythropoietin Treatment in a Rat Model of Focal Ischemia. Stroke, 2009, 40, 936-941.	1.0	62

**GUANGLIANG DING** 

#	Article	IF	CITATIONS
37	Investigation of relationships between transverse relaxation rate, diffusion coefficient, and labeled cell concentration in ischemic rat brain using MRI. Magnetic Resonance in Medicine, 2009, 61, 587-594.	1.9	7
38	Niaspan Treatment Increases Tumor Necrosis Factor-α-Converting Enzyme and Promotes Arteriogenesis after Stroke. Journal of Cerebral Blood Flow and Metabolism, 2009, 29, 911-920.	2.4	33
39	MRI measurement of change in vascular parameters in the 9L rat cerebral tumor after dexamethasone administration. Journal of Magnetic Resonance Imaging, 2008, 27, 1430-1438.	1.9	22
40	Magnetic Resonance Imaging Investigation of Axonal Remodeling and Angiogenesis after Embolic Stroke in Sildenafil-Treated Rats. Journal of Cerebral Blood Flow and Metabolism, 2008, 28, 1440-1448.	2.4	133
41	Quantitative Evaluation of Microvascular Density after Stroke in Rats using MRI. Journal of Cerebral Blood Flow and Metabolism, 2008, 28, 1978-1987.	2.4	31
42	Angiogenesis Detected After Embolic Stroke in Rat Brain Using Magnetic Resonance T2*WI. Stroke, 2008, 39, 1563-1568.	1.0	76
43	Magnetically″abeled sensitized splenocytes to identify glioma by MRI: A preliminary study. Magnetic Resonance in Medicine, 2007, 58, 519-526.	1.9	19
44	Angiogenesis and improved cerebral blood flow in the ischemic boundary area detected by MRI after administration of sildenafil to rats with embolic stroke. Brain Research, 2007, 1132, 185-192.	1.1	108
45	MRI detects white matter reorganization after neural progenitor cell treatment of stroke. NeuroImage, 2006, 32, 1080-1089.	2.1	142
46	MRI of combination treatment of embolic stroke in rat with rtPA and atorvastatin. Journal of the Neurological Sciences, 2006, 246, 139-147.	0.3	19
47	Model Selection in Magnetic Resonance Imaging Measurements of Vascular Permeability: Gadomer in a 9L Model of Rat Cerebral Tumor. Journal of Cerebral Blood Flow and Metabolism, 2006, 26, 310-320.	2.4	119
48	Ischemic Cerebral Tissue Response to Subventricular Zone Cell Transplantation Measured by Iterative Self-Organizing Data Analysis Technique Algorithm. Journal of Cerebral Blood Flow and Metabolism, 2006, 26, 1366-1377.	2.4	32
49	Characterization of cerebral tissue by MRI map ISODATA in embolic stroke in rat. Brain Research, 2006, 1084, 202-209.	1.1	7
50	Detection of BBB disruption and hemorrhage by Gd-DTPA enhanced MRI after embolic stroke in rat. Brain Research, 2006, 1114, 195-203.	1.1	27
51	Analysis of Combined Treatment of Embolic Stroke in Rat with r-tPA and a GPIIb/IIIa Inhibitor. Journal of Cerebral Blood Flow and Metabolism, 2005, 25, 87-97.	2.4	35
52	Quantitative Evaluation of BBB Permeability after Embolic Stroke in Rat Using MRI. Journal of Cerebral Blood Flow and Metabolism, 2005, 25, 583-592.	2.4	63
53	Map-ISODATA demarcates regional response to combination rt-PA and 7E3 F(ab′)2 treatment of embolic stroke in the rat. Journal of Magnetic Resonance Imaging, 2005, 21, 726-734.	1.9	9
54	A Model of Mini-Embolic Stroke Offers Measurements of the Neurovascular Unit Response in the Living Mouse. Stroke, 2005, 36, 2701-2704.	1.0	40

**GUANGLIANG DING** 

#	Article	IF	CITATIONS
55	Multitargeted Effects of Statin-Enhanced Thrombolytic Therapy for Stroke With Recombinant Human Tissue-Type Plasminogen Activator in the Rat. Circulation, 2005, 112, 3486-3494.	1.6	103
56	Early Prediction of Gross Hemorrhagic Transformation by Noncontrast Agent MRI Cluster Analysis After Embolic Stroke in Rat. Stroke, 2005, 36, 1247-1252.	1.0	12
57	Investigation of neural progenitor cell induced angiogenesis after embolic stroke in rat using MRI. NeuroImage, 2005, 28, 698-707.	2.1	151
58	Multiparametric ISODATA analysis of embolic stroke and rt-PA intervention in rat. Journal of the Neurological Sciences, 2004, 223, 135-143.	0.3	29
59	MRI evaluation of treatment of embolic stroke in rat with intra-arterial and intravenous rt-PA. Journal of the Neurological Sciences, 2004, 224, 57-67.	0.3	7
60	In vivo magnetic resonance imaging tracks adult neural progenitor cell targeting of brain tumor. NeuroImage, 2004, 23, 281-287.	2.1	114
61	Magnetic Resonance Imaging Characterization of Hemorrhagic Transformation of Embolic Stroke in the Rat. Journal of Cerebral Blood Flow and Metabolism, 2002, 22, 559-568.	2.4	43
62	Breath-Hold Three-dimensional Contrast-enhanced Coronary MR Angiography: Motion-matched k-Space Sampling for Reducing Cardiac Motion Effects. Radiology, 2000, 215, 600-607.	3.6	23